This is considerably shorter than the observed average period of ~400 ms of the outer vortex line. The effect may be explained by noting that the outer vortex line experiences an additional inward Magnus force due to the countercirculating flow generated by the inner vortex line. Thus, the outer vortex line is not required to move as swiftly to maintain its approximately circumferential motion. (In the presence of an inner vortex line of the same topological charge, the outer vortex line would increase its speed.)

A particularly compelling demonstration of the second, symmetric dipole configuration is shown in Fig. 4. This unusual, time-independent topological structure is a stationary vortex dipole (31–33), the simplest example of a stable vortex cluster in an inhomogeneous superfluid. The stationary vortex dipole arises at the particular vortex separation distance (d_{sep}) at which the Magnus and buoyant forces on each vortex line balance. We find that d_{sep} is essentially constant for $N \sim 4$ to 6×10^5, the range of atomic number in the sequence shown. Averaging the nine measurements of d_{sep} from the images shown in Fig. 4, we find $d_{sep} = 0.432(17) R_\perp^*$. Published predictions for d_{sep} (32, 33) consider only small, weakly interacting systems in two dimensions, unfortunately precluding a straightforward comparison with this measurement.

Small perturbations from the stationary–vortex-dipole configuration are predicted to display a variety of rich behavior, including oscillations of the vortices about their equilibrium positions and a slow precession of the vortices around their axis of symmetry (33). Although a systematic experimental study of this state is difficult due to its low probability of formation, our imaging method can, in principle, be combined with other experimental techniques that consistently generate this or other related (17) topological structures.

Future experiments may examine in detail the dynamics of one-, two-, and many-vortex systems, from their formation during evaporation to their termination at the edge of the condensate (28). For single vortices, the dependence of vortex precession frequencies on the many tunable-system parameters, including temperature and interatomic interaction strength, will permit a close test of theory under a variety of interesting experimental conditions. For vortex dipoles and particularly stationary vortex dipoles, a wealth of predicted interaction dynamics becomes experimentally accessible (33). We expect that dynamical studies of more complicated vortex configurations will be particularly fruitful, from individual vortex motion in disordered arrays to collective behavior in regular lattices (see fig. S1), as well as in the transitions between the two. These fundamental studies promise to deepen our understanding of the important roles that quantized vortices play in diverse superfluid phenomena, including critical-current densities, resistance, and quantum turbulence.

References and Notes
1. D. R. Tilley, J. Tilley, *Superfluidity and Superconductivity* (Institute of Physics Publishing, Philadelphia, ed. 3, 1990).
2. R. J. Donnelly, *Quantized Vortices in Helium II* (Cambridge Univ. Press, New York, 1991).
3. R. E. Packard, *Rev. Mod. Phys.* **70**, 641 (1998).
4. V. B. Eltsov et al., *Phys. Rev. Lett.* **96**, 215302 (2006).
5. V. B. Eltsov et al., *Phys. Rev. Lett.* **99**, 265301 (2007).
6. V. B. Eltsov et al., *Phys. Rev. Lett.* **88**, 065301 (2002).
7. G. P. Bewley, D. P. Lathrop, K. R. Sreenivasan, *Nature* **441**, 588 (2006).
8. K. Harada et al., *Nature* **360**, 51 (1992).
9. M. H. Anderson, J. R. Ensher, M. R. Matthews, C. E. Wieman, E. A. Cornell, *Science* **269**, 198 (1995).
10. K. B. Davis et al., *Phys. Rev. Lett.* **75**, 3969 (1995).
11. C. C. Bradley, C. A. Sackett, J. J. Tollett, R. G. Hulet, *Phys. Rev. Lett.* **75**, 1687 (1995).
12. F. Dalfovo, S. Giorgini, L. P. Pitaevskii, S. Stringari, *Rev. Mod. Phys.* **71**, 463 (1999).
13. P. C. Haljan, B. P. Anderson, I. Coddington, E. A. Cornell, *Phys. Rev. Lett.* **86**, 2922 (2001).
14. P. Engels, I. Coddington, P. C. Haljan, E. A. Cornell, *Phys. Rev. Lett.* **89**, 100403 (2002).
15. B. P. Anderson, P. C. Haljan, C. E. Wieman, E. A. Cornell, *Phys. Rev. Lett.* **85**, 2857 (2000).
16. K. W. Madison, F. Chevy, W. Wohlleben, J. Dalibard, *Phys. Rev. Lett.* **84**, 806 (2000).
17. T. W. Neely, E. C. Samson, A. S. Bradley, M. J. Davis, B. P. Anderson, *Phys. Rev. Lett.* **104**, 160401 (2010).
18. Supporting material is available on *Science* Online.
19. K. M. Mertes et al., *Phys. Rev. Lett.* **99**, 190402 (2007).
20. W. Petrich, M. H. Anderson, J. R. Ensher, E. A. Cornell, *Phys. Rev. Lett.* **74**, 3352 (1995).
21. C. N. Weiler et al., *Nature* **455**, 948 (2008).
22. T. W. B. Kibble, *J. Phys. A Math. Gen.* **9**, 1387 (1976).
23. W. H. Zurek, *Nature* **317**, 505 (1985).
24. V. M. H. Ruutu et al., *Nature* **382**, 334 (1996).
25. V. B. Eltsov, T. W. B. Kibble, M. Krusius, V. M. H. Ruutu, G. E. Volovik, *Phys. Rev. Lett.* **85**, 4739 (2000).
26. A. L. Fetter, *Rev. Mod. Phys.* **81**, 647 (2009).
27. D. S. Rokhsar, *Phys. Rev. Lett.* **79**, 2164 (1997).
28. A. L. Fetter, A. A. Svidzinsky, *J. Phys. Condens. Matter* **13**, R135 (2001).
29. E. A. Burt et al., *Phys. Rev. Lett.* **79**, 337 (1997).
30. F. Dalfovo, M. Modugno, *Phys. Rev. A* **61**, 023605 (2000).
31. L.-C. Crasovan et al., *Phys. Rev. A* **68**, 063609 (2003).
32. M. Möttönen, S. M. M. Virtanen, T. Isoshima, M. M. Salomaa, *Phys. Rev. A* **71**, 033626 (2005).
33. W. Li, M. Haque, S. Komineas, *Phys. Rev. A* **77**, 053610 (2008).
34. We thank J. R. Friedman, R. P. Anderson, and P. G. Kevrekidis for interesting conversations and A. Dewan, E. Altuntas, and A. W. Eddins for experimental assistance. This work was supported by the NSF through grant PHY-0855475.

Plastic Accumulation in the North Atlantic Subtropical Gyre

Kara Lavender Law,[1]* Skye Morét-Ferguson,[1,2] Nikolai A. Maximenko,[3] Giora Proskurowski,[1,2] Emily E. Peacock,[2] Jan Hafner,[3] Christopher M. Reddy[2]

Plastic marine pollution is a major environmental concern, yet a quantitative description of the scope of this problem in the open ocean is lacking. Here, we present a time series of plastic content at the surface of the western North Atlantic Ocean and Caribbean Sea from 1986 to 2008. More than 60% of 6136 surface plankton net tows collected buoyant plastic pieces, typically millimeters in size. The highest concentration of plastic debris was observed in subtropical latitudes and associated with the observed large-scale convergence in surface currents predicted by Ekman dynamics. Despite a rapid increase in plastic production and disposal during this time period, no trend in plastic concentration was observed in the region of highest accumulation.

Plastics are a major contaminant in the world's oceans. Their chemically engineered durability and slow rate of biodegradation (1) allow these synthetic polymers to withstand the ocean environment for years to decades or longer (2). Environmental impacts of ocean plastic are wide-ranging (3) and include entanglement of marine fauna (4), ingestion by seabirds and organisms ranging in size from plankton to marine mammals (4, 5), dispersal of microbial and colonizing species to potentially non-native waters (6, 7), and concentration and transport of organic contaminants to marine organisms at multiple trophic levels (8–10). In the open ocean, the abundance, distribution, and temporal and spatial variability of plastic debris are poorly known, despite an increasing awareness of the problem. Although high concentrations of floating plastic debris have been found in the Pacific Ocean (11–14), only limited data exist to quantify and explain the geographical range and integrated plastic content. In the Atlantic Ocean, the subject has been all but ignored since the earliest studies of marine debris (15–17).

[1]Sea Education Association, Post Office Box 6, Woods Hole, MA 02543, USA. [2]Department of Marine Chemistry and Geochemistry, Woods Hole Oceanographic Institution, 266 Woods Hole Road, Woods Hole, MA 02543, USA. [3]International Pacific Research Center, School of Ocean and Earth Science and Technology, University of Hawai'i, Honolulu, HI 96822, USA.

*To whom correspondence should be addressed. E-mail: klavender@sea.edu

Here, we present an analysis of 22 years of ship-survey data collected in the western North Atlantic Ocean and Caribbean Sea. We examine the abundance, spatial distribution, and temporal variability of plastic debris from samples collected and archived by more than 7000 undergraduate students and faculty scientists at Sea Education Association (SEA) from October 1986 to December 2008. More than 6100 surface plankton net tows were conducted onboard SEA's sailing research vessels, from which more than 64,000 plastic pieces were hand-picked and enumerated (*18*, *19*).

Sixty-two percent of all net tows contained detectable amounts of plastic debris. The highest plastic concentrations were observed between 22° and 38°N (Fig. 1 and figs. S1 and S2), where 83% of total plastic pieces were collected. The largest sample collected in a single 30-min tow was 1069 pieces at 24.6°N, 74.0°W in May 1997, equivalent to 580,000 pieces km^{-2}. The maximum sample size reported in Atlantic studies from the 1970s ranged from 12,000 pieces km^{-2} (*15*) to 167,000 pieces km^{-2} (*16*). Comparatively low plastic concentrations were measured in tows closest to land, such as along the Florida coast and Florida Keys, in the Gulf of Maine, and near Caribbean islands. The average plastic concentration measured within the Caribbean Sea was only 1414 ± 112 pieces km^{-2}, while that in the Gulf of Maine was 1534 ± 200 pieces km^{-2}, both more than an order of magnitude lower than the average concentration near 30°N (20,328 ± 2324 pieces km^{-2}, 29° to 31°N). Although in our study region the latitudinal bounds of the highest plastic concentration are well defined, the eastern extent has not yet been determined because of a lack of direct observations.

The region of highest plastic concentration is clearly associated with the large-scale subtropical convergence in the surface velocity field created by wind-driven Ekman currents and geostrophic circulation (Fig. 2). This convergence zone, indicated by converging streamlines and current velocities less than 2 cm s^{-1}, extends across most of the subtropical North Atlantic basin (*20*) and coincides with the highest observed plastic concentrations. This correspondence not only explains the plastic distribution but also illustrates how floating debris acts as a tracer of large-scale mean surface currents.

While the convergence acts to concentrate floating debris, the geographic origin of the debris cannot be easily determined from current patterns or from the recovered plastic samples themselves. To address this question, we used data from satellite-tracked drifting surface buoys (drifters) (*21*) to examine pathways into and out of the "central region" of high plastic concentration (26° to 34°N, 60° to 70°W). Of 1666 drifters broadly deployed in the North Atlantic (0° to 76°N, 0° to 90°W) from 1989 to 2009, 24 drifters were deployed in the central region and 116 others passed through this region. The trajectories of these "central region" drifters were strongly con-

fined to the western subtropical gyre; before entering the central region, 66% (92 drifters) originated west of 50°W and between 18° and 42°N, whereas only 10% (14 drifters) ultimately drifted outside of this area (fig. S3). This suggests that floating plastic debris, similarly transported by surface currents, may have originated in the subtropical western North Atlantic where currents also act to retain it. This is further supported by a numerical model based on drifter statistics (*22*). The model was initialized with a homogeneous concentration of a passive tracer and integrated forward in time. After 10 years, the tracer converged in the North Atlantic subtropical gyre with a maximum concentration 15 times its initial value. This convergence, centered at approximately 30°N, directly corresponds to the observed high plastic accumulation region (fig. S2).

Further, the model indicates that the minimum time for surface tracer (i.e., drifter or plastic) to reach the collection center from the U.S. eastern seaboard is less than 60 days, at least half the time required to travel from Europe or Africa. The influence of the Gulf Stream is particularly evident in some of the fastest propagation times—40 days from Washington, D.C., and Miami, Florida, for example—in which tracer traveled along the coast before entering the gyre interior. Although not indicative of the size or location of land-based sources, or of the age of debris, these estimates demonstrate how quickly plastic entering the ocean near major U.S. population centers could affect an area more than 1000 km offshore.

We observed no strong temporal trends in plastic concentration in the 22-year data set (Fig. 3). Large interannual variability was observed within the high plastic concentration region, and a linear fit to annual mean plastic concentration had a slope not different from zero (–20 ± 217 pieces

km^{-2} year^{-1}; $r^2 = 0.00$, $P > 0.1$). Although the average concentration in this region did show a statistically significant increase from the 1990s to 2000s ($P = 0.0097$, 962 DOF), this increase disappeared when concentrations greater than 200,000 pieces km^{-2} (less than 1% of values) were removed ($P = 0.6947$, 1382 DOF). To address a potential sampling bias, the analysis was also performed with data from the most spatially consistent, annually repeated cruise track from Woods Hole, Massachusetts, to St. Croix, U.S. Virgin Islands. In this case, a weak but not statistically significant decreasing trend (–573 ± 265 pieces km^{-2} year^{-1}; $r^2 = 0.21$, $P > 0.1$) was observed in the high plastic concentration region (fig. S4). Although the nonuniform sampling in this data set cannot resolve short spatial or temporal scale variability, no robust trend was observed in the broadest region of plastic accumulation on interannual time scales and longer.

Although no direct estimates of plastic input to the ocean exist, the increase in global production of plastic materials [fivefold increase from 1976 to 2008 (*23*)] together with the increase in discarded plastic in U.S. municipal solid waste (MSW) [fourfold increase from 1980 to 2008 (*24*) (Fig. 3)] suggest that the land-based source of plastic into the ocean increased during the study period. Ocean-based sources may have decreased in response to international regulations prohibiting dumping of plastic at sea (*25*). Given the measured steady plastic concentration in the western North Atlantic, loss terms must exist to offset the presumed increase in plastic input to the ocean.

A change in the type of plastic material entering the ocean could affect the observed amount of floating debris. Density analysis of plastic samples collected at the sea surface revealed that 99% were less dense than seawater, and ele-
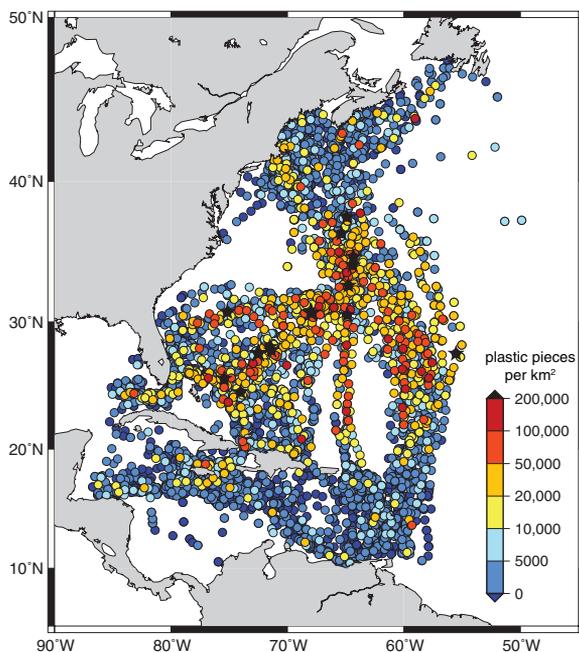
Fig. 1. Distribution of plastic marine debris collected in 6136 surface plankton net tows on annually repeated cruise tracks from 1986 to 2008 in the western North Atlantic Ocean and Caribbean Sea. Symbols indicate the location of each net tow; color indicates the measured plastic concentration in pieces km^{-2}. Black stars indicate tows with measured concentration greater than 200,000 pieces km^{-2}. Symbols are layered from low to high concentration.

plastic pieces per km²
200,000
100,000
50,000
20,000
10,000
5000
0

mental analysis indicated properties consistent with the buoyant plastic materials high- and low-density polyethylene, and polypropylene (26). Between 1993 and 2008, a 24% increase in discarded buoyant plastics was estimated in U.S. MSW, totaling 14.5 million tons in 2008 (24, 27). Assuming that plastic input into the ocean followed a similar trend, a measurable increase in floating plastic is expected.

Industrial resin pellets, the "raw material" of consumer plastic products, are an additional source of plastic to the ocean. In 1991, in response to a U.S. Environmental Protection Agency (EPA) study (28), the plastics industries voluntarily instituted a program to prevent or recapture spilled pellets (29). Between 1986 and 2008, we observed a statistically significant decrease in the average concentration of resin pellets in the entire region sampled (-32 ± 4 pieces km^{-2} year^{-1}; $r^2 = 0.79$, $P < 0.01$); however, the pellet concentration was only a small fraction of the total plastic material

collected (annually averaged concentration ranged from 200 to 1000 pellets km^{-2}, or 1 to 16% of total pieces). This trend suggests that efforts to reduce plastic input at a land-based source may be measurably effective.

Spatial and temporal variability in surface ocean currents could result in an export of debris from the high concentration region in anomalous currents or eddies, or could alter the distribution through a shift in the large-scale circulation pattern. The convergence of modeled tracer into the subtropical gyre suggests a long residence time (10 to 100 years) (22), and therefore a relatively small removal by anomalous currents. Long-term shifts in the large-scale circulation pattern are driven by changes in wind forcing. Surface wind estimates (30) during three intervals spanning the study period (1988 to 1992, 1995 to 1999, and 2004 to 2008) showed only small variations in wind speed and direction across the North Atlantic. Therefore, it is unlikely that ocean circula-
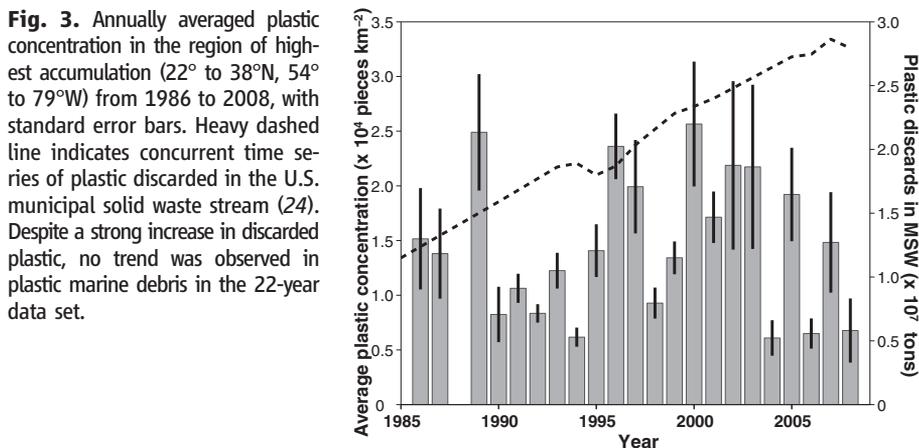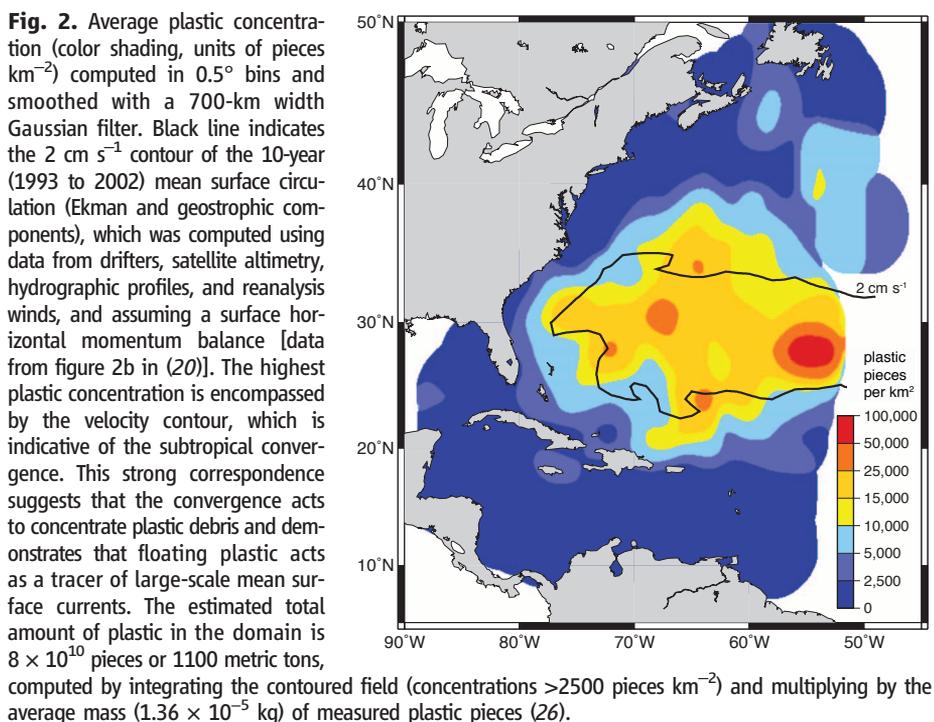
tion could account for an export of plastic from the region large enough to offset the presumed increase in input.

Possible sinks for floating plastic debris include fragmentation, sedimentation, shore deposition, and ingestion by marine organisms. In the marine environment, photodegradation and oxidative and hydrolytic degradation cause many common plastics to become embrittled and suffer mechanical breakdown on time scales of months (31, 32). Analysis of a subset of samples (26) indicated that 88% were less than 10 mm in largest dimension, and most had characteristics suggesting physical deterioration such as brittleness, rough edges, or cracks. It is likely that plastic pieces ultimately become small enough to pass through the 335-μm mesh net used in this study, although the rate of mechanical degradation is not expected to vary on the time scale of the study.

In ocean conditions, the density of buoyant plastic debris may increase over time due to rapid biofilm formation and subsequent aggregation of fouling organisms (26, 33). Elemental analysis of plastic samples revealed the presence of nitrogen (26), which is absent in virgin polyethylenes and polypropylene and thus indicative of bioaccumulation. The fate of plastic particles that become dense enough to sink below the sea surface is unknown, and we are unaware of any studies of seafloor microplastics offshore of the continental shelf. However, analysis of particle trap data in the center of the high plastic region near Bermuda shows no evidence of plastic as a substantial contributor to trapped sinking material at depths of 500 to 3200 m (34).

Plastic debris is a common feature of beaches on the U.S. east coast (26, 35) and on island beaches in Bermuda (17, 36) and the Bahamas (17). However, there are no published records of temporal trends in island beach deposition, and 10-year records from U.S. east coast beaches show regionally variable seasonal and long-term trends in marine debris (35). Finally, ingestion of plastic debris has been well documented in seabirds and large marine animals (4), and manipulative feeding experiments have revealed ingestion of microplastics by much smaller organisms (5, 37). Because the cohort of pelagic organisms that ingest plastic, their ingestion rates, and the fate of ingested plastics are unknown, it is impossible to estimate the size of this sink.

A study of plastic microdebris in waters from the British Isles to Iceland (5) revealed a statistically significant increase in plastic abundance from the 1960s and 1970s to the 1980s and 1990s. However, similar to this study, no significant increase was observed between the later decades despite a large increase in plastic production and disposal. Together, our studies illustrate how poorly constrained are the sources and sinks of plastic debris in the ocean. The 22-year data set presented here provides evidence that floating plastic debris acts as a passive tracer of ocean circulation, accumulating in the large-scale subtropical

Fig. 2. Average plastic concentration (color shading, units of pieces km^{-2}) computed in 0.5° bins and smoothed with a 700-km width Gaussian filter. Black line indicates the 2 cm s^{-1} contour of the 10-year (1993 to 2002) mean surface circulation (Ekman and geostrophic components), which was computed using data from drifters, satellite altimetry, hydrographic profiles, and reanalysis winds, and assuming a surface horizontal momentum balance [data from figure 2b in (20)]. The highest plastic concentration is encompassed by the velocity contour, which is indicative of the subtropical convergence. This strong correspondence suggests that the convergence acts to concentrate plastic debris and demonstrates that floating plastic acts as a tracer of large-scale mean surface currents. The estimated total amount of plastic in the domain is 8×10^{10} pieces or 1100 metric tons, computed by integrating the contoured field (concentrations >2500 pieces km^{-2}) and multiplying by the average mass (1.36×10^{-5} kg) of measured plastic pieces (26).

Fig. 3. Annually averaged plastic concentration in the region of highest accumulation (22° to 38°N, 54° to 79°W) from 1986 to 2008, with standard error bars. Heavy dashed line indicates concurrent time series of plastic discarded in the U.S. municipal solid waste stream (24). Despite a strong increase in discarded plastic, no trend was observed in plastic marine debris in the 22-year data set.

convergence as predicted by ocean physics. This analysis provides an important baseline for future monitoring efforts, as well as a quantitative assessment to accurately inform the public and policymakers of the scope of this environmental problem.

References and Notes

1. M. Sudhakar et al., Polym. Degrad. Stabil. **92**, 1743 (2007).
2. D. Shaw, R. Day, Mar. Pollut. Bull. **28**, 39 (1994).
3. M. R. Gregory, Philos. Trans. R. Soc. London Ser. B **364**, 2013 (2009).
4. D. W. Laist, Mar. Pollut. Bull. **18**, 319 (1987).
5. R. C. Thompson et al., Science **304**, 838 (2004).
6. H. Webb, R. Crawford, T. Sawabe, E. Ivanova, Microbes Environ. **24**, 39 (2009).
7. D. K. Barnes, Nature **416**, 808 (2002).
8. Y. Mato et al., Environ. Sci. Technol. **35**, 318 (2001).
9. E. L. Teuten, S. J. Rowland, T. S. Galloway, R. C. Thompson, Environ. Sci. Technol. **41**, 7759 (2007).
10. E. L. Teuten et al., Philos. Trans. R. Soc. London Ser. B **364**, 2027 (2009).
11. C. S. Wong, D. R. Green, W. J. Cretney, Nature **247**, 30 (1974).
12. D. G. Shaw, G. A. Mapes, Mar. Pollut. Bull. **10**, 160 (1979).
13. R. H. Day, D. G. Shaw, Mar. Pollut. Bull. **18**, 311 (1987).
14. R. H. Day, D. G. Shaw, S. E. Ignell, The quantitative distribution and characteristics of marine debris in the North Pacific Ocean, 1984–88. Proceedings of the Second International Conference on Marine Debris U.S. Dept. Commerce, NOAA Tech. Memo NOAA-TM-NMFS-SWFCC-154, pp. 182–211 (1990).
15. E. J. Carpenter, K. L. Smith Jr., Science **175**, 1240(1972).
16. J. B. Colton Jr., B. R. Burns, F. D. Knapp, Science **185**, 491 (1974).
17. R. J. Wilber, Oceanus **30**, 61 (1987).
18. Materials and methods are available as supporting material on Science Online.
19. The 22-year data set has been deposited with the Marine Geoscience Data System, www.marine-geo.org/tools/
search/entry.php?id=NorthAtlantic_Law, and is also available at www.geomapapp.org.
20. N. Maximenko et al., J. Atmos. Ocean. Technol. **26**, 1910 (2009).
21. Drifters are drogued at 15-m depth; only those whose drogue was attached for its full lifetime were used in this analysis. Data courtesy of (38).
22. International Pacific Research Center, Tracking ocean debris. IPRC Climate **8**, 14 (2008) (http://iprc.soest.hawaii.edu/newsletters/iprc_climate_vol8_no2.pdf).
23. PlasticsEurope Market Research Group, The Compelling Facts About Plastics 2009 (PEMRG, Brussels, Belgium, 2009); www.plasticseurope.org/Documents/Document/20100225141556-Brochure_UK_FactsFigures_2009_22sept_6_Final-20090930-001-EN-v1.pdf.
24. U.S. Environmental Protection Agency, Municipal Solid Waste Generation, Recycling, and Disposal in the United States: Detailed Tables and Figures for 2008 (EPA, Washington, DC, 2009); www.epa.gov/osw/nonhaz/municipal/msw99.htm.
25. International Convention for the Prevention of Pollution from Ships (MARPOL), Annex V: Prevention of Pollution by Garbage from Ships (1988); www.imo.org/Environment/mainframe.asp?topic_id=297
26. S. Morét-Ferguson et al., Mar. Pollut. Bull. 10.1016/j.marpolbul.2010.07.020 (2010).
27. Polystyrene foam is buoyant in seawater, but solid polystyrene is not. The U.S. EPA report does not distinguish between the two forms; thus, polystyrene was not included in the calculation. Discarded polystyrene in MSW increased 6% from 1993 to 2008.
28. U.S. Environmental Protection Agency, Plastic Pellets in the Aquatic Environment: Sources and Recommendations: Final Report (EPA 842-S-93-001) (EPA, Washington, DC, 1993); www.epa.gov/owow/oceans/debris/plasticpellets/plasticpellets.pdf.
29. American Chemistry Council, Operation Clean Sweep Pellet Handling Manual (www.opcleansweep.org).
30. National Centers for Environmental Prediction reanalysis data are provided by the NOAA/OAR/ESRL PSD, Boulder, CO, USA, and are available at www.esrl.noaa.gov/psd.
31. A. Andrady, J. Appl. Polym. Sci. **39**, 363 (1990).
32. D. Feldman, J. Polym. Env. **10**, 163 (2002).
33. S. Ye, A. Andrady, Mar. Pollut. Bull. **22**, 608 (1991).
34. Since 2003, routine analysis of particle trap data from the Oceanic Flux Program time series (39) has found no evidence of the presence of microplastic either in visual analysis using stereo microscopy for fractions >125 μm or in carbon-to-nitrogen ratios for the <125-μm size fraction.
35. C. A. Ribic, S. B. Sheavly, D. J. Rugg, E. S. Erdmann, Mar. Pollut. Bull. **60**, 1231 (2010).
36. M. Gregory, Mar. Environ. Res. **10**, 73 (1983).
37. E. R. Graham, J. T. Thompson, J. Exp. Mar. Biol. Ecol. **368**, 22 (2009).
38. Global Drifter Program, www.aoml.noaa.gov/phod/dac/gdp.html.
39. Oceanic Flux Program time series; http://ecosystems.mbl.edu/conte/ofp/index.html.
40. We thank the thousands of students and staff at Sea Education Association who collected plastic samples onboard the research vessel Westward and the sailing school vessel Corwith Cramer. This work was supported by the National Science Foundation (OCE-0842727) and the Hollis and Ermine Lovell Charitable Foundation. N.A.M. and J.H. were supported by the National Fish and Wildlife Foundation (2008-0066-006); the NASA Physical Oceanography Program through membership in its Ocean Surface Topography Science Team (NNX08AR49G); and the Japan Agency for Marine-Earth Science and Technology (JAMSTEC), NASA (NNX07AG53G), and the National Oceanic and Atmospheric Administration (NA17RJ1230), which sponsor research at the International Pacific Research Center.

Graphene Visualizes the First Water Adlayers on Mica at Ambient Conditions

Ke Xu,*† Peigen Cao,* James R. Heath‡

The dynamic nature of the first water adlayers on solid surfaces at room temperature has made the direct detection of their microscopic structure challenging. We used graphene as an atomically flat coating for atomic force microscopy to determine the structure of the water adlayers on mica at room temperature as a function of relative humidity. Water adlayers grew epitaxially on the mica substrate in a layer-by-layer fashion. Submonolayers form atomically flat, faceted islands of height 0.37 ± 0.02 nanometers, in agreement with the height of a monolayer of ice. The second adlayers, observed at higher relative humidity, also appear icelike, and thicker layers appear liquidlike. Our results also indicate nanometer-scale surface defects serve as nucleation centers for the formation of both the first and the second adlayers.

Water coats all hydrophilic surfaces under ambient conditions, and the first water adlayers on a solid often dominate the surface behavior (1–4). Although scanning tunneling microscopy (STM) and other ultrahigh vacuum surface characterization techniques have been extensively used to study water (ice) adlayers on solids at cryogenic temperatures (1, 2), such techniques are not applicable to room-temperature studies because of the high vapor pressure of water (2, 3). Various optical methods have been used at ambient conditions to probe the averaged properties of water adlayers over macroscopic areas (3, 5–7). Atomically resolved studies have remained challenging. For example, although thin ice layers have been studied with atomic force microscopy (AFM) below freezing temperatures (8, 9), reliable AFM imaging of water adlayers under ambient conditions is confounded by tip-sample interactions (2). For example, the capillary menisci formed between the tip and the sample strongly perturb the water adlayers on solids (10).

Scanning polarization force microscopy (SPFM) has been used to image water adlayers (2, 11, 12). For SPFM, the tip-sample distance is kept at tens of nanometers. By briefly contacting the tip on a mica surface to induce capillary condensation, metastable islandlike structures were observed in SPFM images. These islands were interpreted as a second adlayer on a monolayer of water (2, 12). However, the lateral resolution of SPFM is relatively low, and the measured apparent heights reflect local polarizability instead of actual heights. Furthermore, the structure of the first adlayer was not observed, likely because of the low lateral resolution and/or the dynamic nature of the first adlayer (12).

Kavli Nanoscience Institute and Division of Chemistry and Chemical Engineering, California Institute of Technology, MC 127-72, Pasadena, CA 91125, USA.

*These authors contributed equally to this work.
†Present address: Department of Chemistry and Chemical Biology, Harvard University, 12 Oxford Street, Cambridge, MA 02138, USA.
‡To whom correspondence should be addressed. E-mail: heath@caltech.edu